Monaldi Arch Chest Dis
2005; 63: 1, 59-64

CASE REPORT

Pulmonary Alveolar Microlithiasis: CT and pathologic findings in 10 patients

H. Sumikawa[1], T. Johkoh[1, 2], N. Tomiyama[1], S. Hamada[1], M. Koyama[1], M. Tsubamoto[1], S. Murai[1], A. Inoue[1], H. Nakamura[1], T. Tachibana[3], N.L. Müller[4]

ABSTRACT: ***Pulmonary Alveolar Microlithiasis: CT and pathologic findings in 10 patients. H. Sumikawa, T. Johkoh, N Tomiyama, S. Hamada, M. Koyama, M. Tsubamoto, S. Murai, A. Inoue, H. Nakamura, T. Tachibana, N.L. Müller.***

Background and Aim. **To evaluate CT findings of pulmonary alveolar microlithiasis and correlate the CT with the pathologic findings.**

Methods. **The study included 10 patients with pathologically proven microlithiasis. Two independent observers evaluated the presence, extent and distribution of the CT findings. CT findings were compared with those at autopsy in two patients and with transbronchial biopsy in eight patients.**

Results. **All patients had a myriad of calcified nodules measuring approximately 1 mm in diameter. Close apposition of the nodules resulted in areas of ground-glass attenuation and consolidation, which were the predominant abnormality on CT in all 10 patients, involving 41% ± 16.3 (mean ± SD) and 30% ± 4.8 of the lung parenchyma, respectively. Calcifications were also seen along interlobular septa, bronchovascular bundles and pleura. Other findings included interlobular septal thickening, thickening of bronchovascular bundles, nodules, and subpleural cysts. There was a solid agreement between the observers for the presence (kappa value; 0.77) and extent (Spearman rank correlation; r= 0.81 to 1.0 p<0.01) of abnormalities. Autopsy specimens demonstrated microliths in alveolar airspaces and along interlobular septa, bronchovascular bundles and pleura. Subpleural small cysts were shown to represent dilated alveolar ducts.**

Conclusion. **Pulmonary microlithiasis is characterised by the presence of numerous small, calcified nodules, calcifications along interlobular septa, bronchovascular bundles and pleura, ground-glass opacities, consolidation, and subpleural cysts. The cysts represent dilated alveolar ducts.**
Monaldi Arch Chest Dis 2005; 63: 1, 59-64.

Keywords: Microlithiasis, CT, lung, diffuse lung disease, calcification.

[1] Department of Radiology, Osaka University Graduate School of Medicine,
[2] Department of Medical Physics, Osaka University Graduate School of Medicine,
[3] Department of Internal Medicine, Osaka Kampo Medical Center, Japan
[4] Department of Radiology, University of British Columbia and Vancouver Hospital and Health Sciences Center, Canada.

Correspondence Dr. Hiromitsu Sumikawa, Department of Radiology, Osaka University Graduate School of Medical, 2-2 Yamadaoka, Suita, Osaka, 565-0825, Japan; e-mail: h-sumikawa@radiol.med.osaka-u.ac.jp

Introduction

Pulmonary alveolar microlithiasis is a rare disease characterised by widespread intra-alveolar accumulation of calcium phosphate, which form characteristically, small nodular laminated calcospherites. Many patients are asymptomatic at presentation, the disease being discovered incidentally on a chest radiograph [1, 2]. The radiographic pattern is a characteristic consisting of fine sand-like micronodulation throughout both lungs, which often obliterates the mediastinal and diaphragmatic contour [2].

The CT descriptions have been limited to a small number of patients, mainly in the form of isolated case reports [3-7]. The CT findings have been reported as consisting of tiny calcific nodules mainly in the dependent portion of the lower lung zones. Less common reported findings include apparent calcification of the interlobular septa and subpleural cysts. The aim of this study was to evaluate CT findings of pulmonary alveolar microlithiasis in 10 patients and correlate them with pathologic findings.

Methods

Seven women and three men (mean age, 51 years; age range, 41-72 years) who had pathological diagnosis of pulmonary alveolar microlithiasis and had undergone CT of the chest were included in the study. Pathological diagnosis was obtained at transbronchial biopsy in eight patients and at autopsy in two patients.

In all patients, continuous 10-mm collimation CT scans were performed from apex to lung bases using a standard algorithm. In three patients, three to five thin section CT images were performed using 1 to 2-mm collimation and reconstructed using a high spatial frequency algorithm. All images were photographed at a lung window setting level -600 to -700 HU, width 1000 to 1500 HU. In order

to observe the appearance of calcification, special window settings (level -400 to 150 HU and width 1000 to 4000 HU) were also used. The CT scans were performed on a variety of scanners. None of the patients received intravenous contrast medium.

The CT images were reviewed independently by two observers. The lungs were divided into three zones (upper, middle, and lower); each zone was evaluated separately. Each of the three zones corresponded to approximately one-third of the images from the lung apex to 1 cm below the domes of the diaphragm.

The observers assessed the presence, extent, and distribution of nodules, areas of ground-glass attenuation, consolidation, interlobular septal thickening, thickening of bronchovascular bundles, intralobular reticular opacity, traction bronchiectasis, emphysema, cysts, lymph node enlargement, pleural thickening and pleural effusion. The presence of calcifications of normal anatomic structures in each lung was also assessed.

Ground-glass attenuation was defined as an area of hazy increased attenuation without obscuration of underlying vascular markings. Consolidation was considered present when the opacity obscured the underlying vessels. Traction bronchiectasis was defined as irregular bronchial dilatation within areas with parenchymal abnormalities. Lymph nodes were considered enlarged if the short-axis diameter at CT was greater than 10 mm.

The anatomic distribution was noted to be central if there was a predominance of abnormalities in the inner two-thirds of the lung, peripheral if there was a predominance of abnormalities in the outer third of the lung, dorsal if there was predilection for the dependent portion, peribronchovascular if there was predilection for the peribronchovascular areas, and random if there was no predominance. Upper lung zone predominance was considered present when most of the abnormalities were above the level of the tracheal carina, and lower zone predominance was considered present when most of the abnormalities were below this level.

The extent of involvement of each abnormality was assessed independently for each of three zones of each lung. The CT score in upper, middle, and lower lung zones was determined by visually estimating the extent of disease in each zone. The score was based on the percentage of lung parenchyma that showed evidence of abnormality and was estimated to the nearest 10% of parenchymal involvement. The overall percentage of involvement was obtained by averaging the six lung zones.

The extent of traction bronchiectasis was evaluated counting the number of pulmonary segments that showed traction bronchiectasis and by assessing the generations of bronchial divisions involved. Traction bronchiectasis was scored as follows: 0, no bronchial dilatation; 1, dilatation limited to bronchi distal to the sixth-generation bronchi, the main bronchi being considered the first generation; 2, bronchial dilatation involving the fifth-generation bronchi; 3, bronchial dilatation involving the fourth generation; 4, bronchial dilatation involving the third generation; and 5, bronchial dilatation involving bronchi proximal to the second generation. In eight patients the transbronchial biopsy results were reviewed and in two patients the CT findings were correlated with the findings on the autopsy specimens.

The interobserver variation of the extent of various abnormalities was evaluated with the Spearman's rank correlation coefficient. The interobserver variation of the existence of predominant distribution, architectural distortion, lymph node enlargement and pleural effusion was analyzed by using kappa statistics. The inter-observer agreement was classified as follows: poor, κ = 0-0.20; fair, κ = 0.21-0.40; moderate, κ = 0.41-0.60; good, κ = 0.61-0.80; and excellent, κ = 0.81-1.00.

Results

CT findings

There was a solid inter-observer agreement for the extent of the various abnormalities (Spearman's rank correlation coefficient, r = 0.81 to 1.0, $p<0.01$) and for the presence of predominant distribution, architectural distortion, lymph node enlargement and pleural effusion (κ = 0.77). Therefore, the description of the CT findings is based on the average of the observations made by two observers.

All patients had innumerous calcified nodules measuring approximately 1 mm in diameter (table 1). Close apposition of the nodules resulted in areas of ground glass attenuation and consolidation, which were the predominant abnormality on CT in all 10 patients (fig. 1). The areas with ground-glass attenuation and consolidation involved 41% ± 16.3

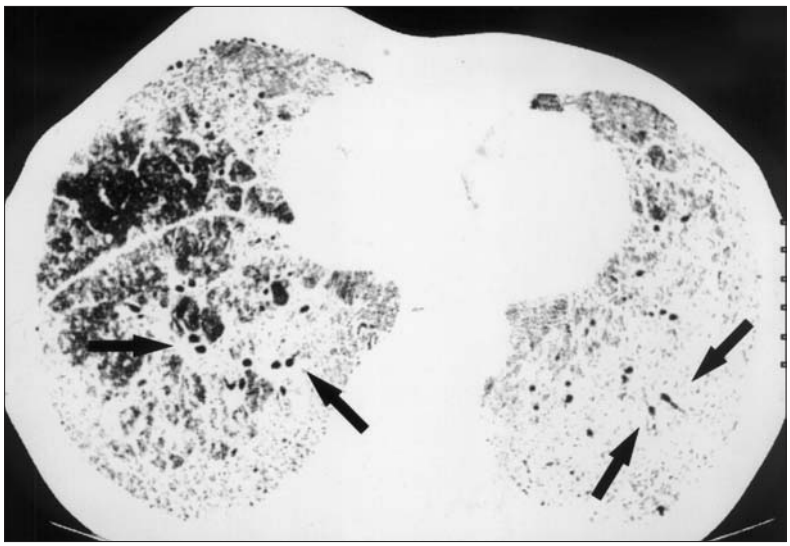

Fig. 1. - A 55-year-old man (window level -700, window width 1000, slice thickness 10 mm). CT image shows small calcified nodules, ground-glass opacities and consolidation. Air bronchograms can be seen in the areas of consolidation (arrows).

Table 1. - Mean Number of Patients with CT Findings Under review and Mean CT Extent of Findings

CT findings	Number of cases	Extent in all cases	The interobserver variation	
			r Value	p Value
Ground-glass attenuation	10*	41.6 ± 16.3†	0.942	<0.01
Consolidation	10*	29.1 ± 4.82†	0.891	<0.01
Calcified 1 mm nodules	10*	12.8 ± 4.57†	0.933	<0.01
Interlobular septal thickening	10*	16.3 ± 5.96†	0.921	<0.01
Thickening of bronchovascular bundles	10*	14.4 ± 6.91†	0.955	0.04
Pleural thickening	7*	10.1 ± 12.1†	0.806	0.02
Intralobular reticular opacity	6*	4.08 ± 3.44†	0.942	<0.01
Honeycombing	0*	0†	1	<0.01
Cyst	10*	11.2 ± 3.55†	0.897	<0.01
Emphysema	1*	0.17 ± 0.75†	0.864	<0.01
Traction bronchiectasis	10*	14.1 ± 448‡	1	<0.01
Generation of bronchial divisions involved by traction bronchiectasis	10*	3.2 ± 1.14§	1	<0.01

* Number of patients with each abnormality; † Mean percentage of lung parenchyma ± SD; ‡ Mean number of segments or subsegments ± SD; § Mean scores ± SD. Scores are defined in Materials and Methods.

(mean ± SD) and 30% ± 4.8 of the lung parenchyma, respectively. Interlobular septal thickening, thickening of bronchovascular bundles, cysts, traction bronchiectasis, lymphadenopathy and architectural distortion were present in all patients (table 1). Interlobular septal thickening and thickening of bronchovascular bundles was present in 16.3 ± 5.96 and 14.4 ± 6.91 of the lung parenchyma, respectively (fig. 2).

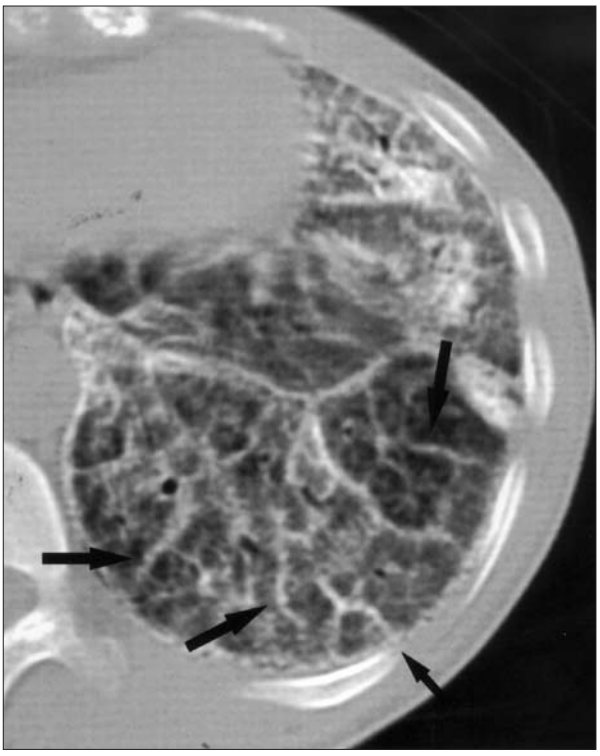

Fig. 2. - A 41-year-old woman (window level -400, window width 4000, slice thickness 10 mm).
CT scan through the left lower lobe demonstrates thickening of interlobular septa (arrows) and evidence of calcification of the interlobular septa. Also noted are small nodules and parenchymal calcification due to apposition of numerous nodules.

The vast majority of nodules were approximately 1 mm in diameter and all nodules were smaller than 1 cm in diameter. The majority of nodules had a random distribution, some had a predominant centrilobular or subpleural distribution, and some showed a predominant distribution along interlobular septa and bronchovascular bundles. All patients had thin-walled cysts, measuring less than 1cm in diameter, distributed along the pleura [fig. 3 (A)]. Five patients had apical bullae.

Calcification was present in the nodules, along interlobular septa, pleura, and bronchovascular bundles. The areas of air-space consolidation were diffusely calcified and contained air bronchograms (fig. 1, 4). Calcifications along pleura resulted in calcified lines, which were present on CT in 9 of the 10 patients. The lines were most prominent along the mediastinal pleura [fig. 3 (A)].

Lower lung zone predominance was present in five patients, and no zonal predominance was seen in five. In all cases the calcifications involved mainly the dependent lung regions.

CT-Pathologic correlation

Histological assessment of transbronchial and autopsy specimens showed filling of the alveolar airspaces with calcospherites. The vast majority of the calcific nodules measured less than 1 mm in diameter. The limited size of the transbronchial specimens did not allow assessment of distribution of nodules in the interstitium. The autopsy specimens available in two patients demonstrated calcification along interlobular septa, bronchovascular bundles and pleura [fig. 3 (B)]. Ground-glass opacification and consolidation on CT was shown to be due to the apposition of a myriad of calcospherites. Apparent pleural calcification (calcified pleural lines) on the CT was shown to be due mainly to the presence of numerous calcified nodules in the subpleural lung parenchyma. Autopsy

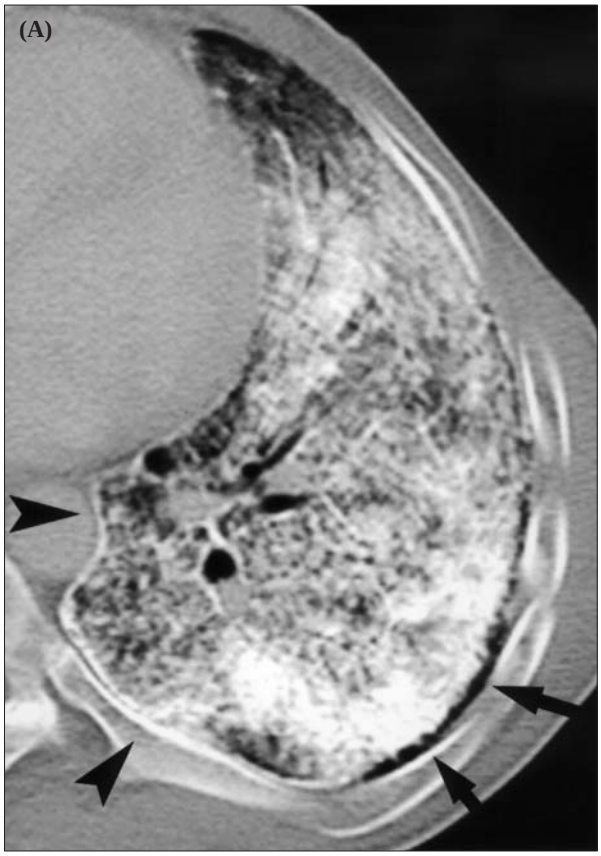

Fig. 3. - A 49-year-old man (window level 155, window level 1858, slice thickness 10 mm).
(A) CT scan through left lower lobes demonstrates small cysts along the pleura (arrows). Also note calcific line in the mediastinal pleura (arrowheads).
(B) Histologic section. Hematoxylin-eosin stain. (original magnification, x16) Many microliths are present along the pleura (arrow heads), which is not calcified. Most distal alveolar ducts are dilated (arrows).

specimens demonstrated only small amounts of pleural calcification. Sub-pleural small cysts seen on CT and on the gross lung specimens were shown histologically to represent dilated alveolar ducts [fig. 3 (B)]. The two lung specimens also showed mild interstitial fibrosis.

Discussion

Pulmonary alveolar microlithiasis is a rare chronic disease characterised by the deposition of calcium phosphate microliths in the alveolar airspaces. The etiology is unknown but the high rate of occurrence within families suggests an autosomal-recessive hereditary nature [8]. Many patients are initially asymptomatic even in the presence of fairly extensive abnormalities on the chest radiograph. The disease is slowly progressive resulting in progressive dyspnea and, eventually, in respiratory failure [9]. The diagnosis can often be suggested based on the findings on the chest radiograph, but transbronchial or surgical biopsy are necessary for final diagnosis [10]. Sometimes, calcospherites can be found in the sputum or in bronchoalveolar lavage fluid [11].

There are several reports on the findings of pulmonary alveolar microlithiasis from chest radiography [1, 2, 12]. The characteristic radiographic manifestation consists of bilateral fine sand-like micronodulation of calcific densities involving mainly the middle and lower zones. The individual deposits are usually identifiable as sharply defined nodules measuring 1 mm or less in diameter [1, 2, 12]. The description of the CT findings have been based largely on individual case reports [2-6]. CT findings have been reported as consisting of small nodular calcific densities, which are often confluent and diffusely distributed throughout the lung.

The present study demonstrates that apposition of numerous small, calcified nodules results in areas of ground-glass attenuation and consolidation, which were the predominant finding in all patients. Areas of air-space consolidation were diffusely calcified. In the areas with ground-grass attenuation, small, calcified dots were seen. Therefore, as confirmed on the correlation of CT with the histologic findings, areas of ground-glass attenuation and consolidation resulted from apposition of a myriad of microliths.

Miro et al. reported a case of alveolar microlithiasis characterised by a reticulonodular pattern with Kerley B lines and *Melamed et al*. reported a case in which interstitial thickening was prominent on high-resolution CT [13, 14]. Interlobular septal thickening and thickening of bronchovascular bundles as well as calcified nodules along these structures were seen in all patients in the current study.

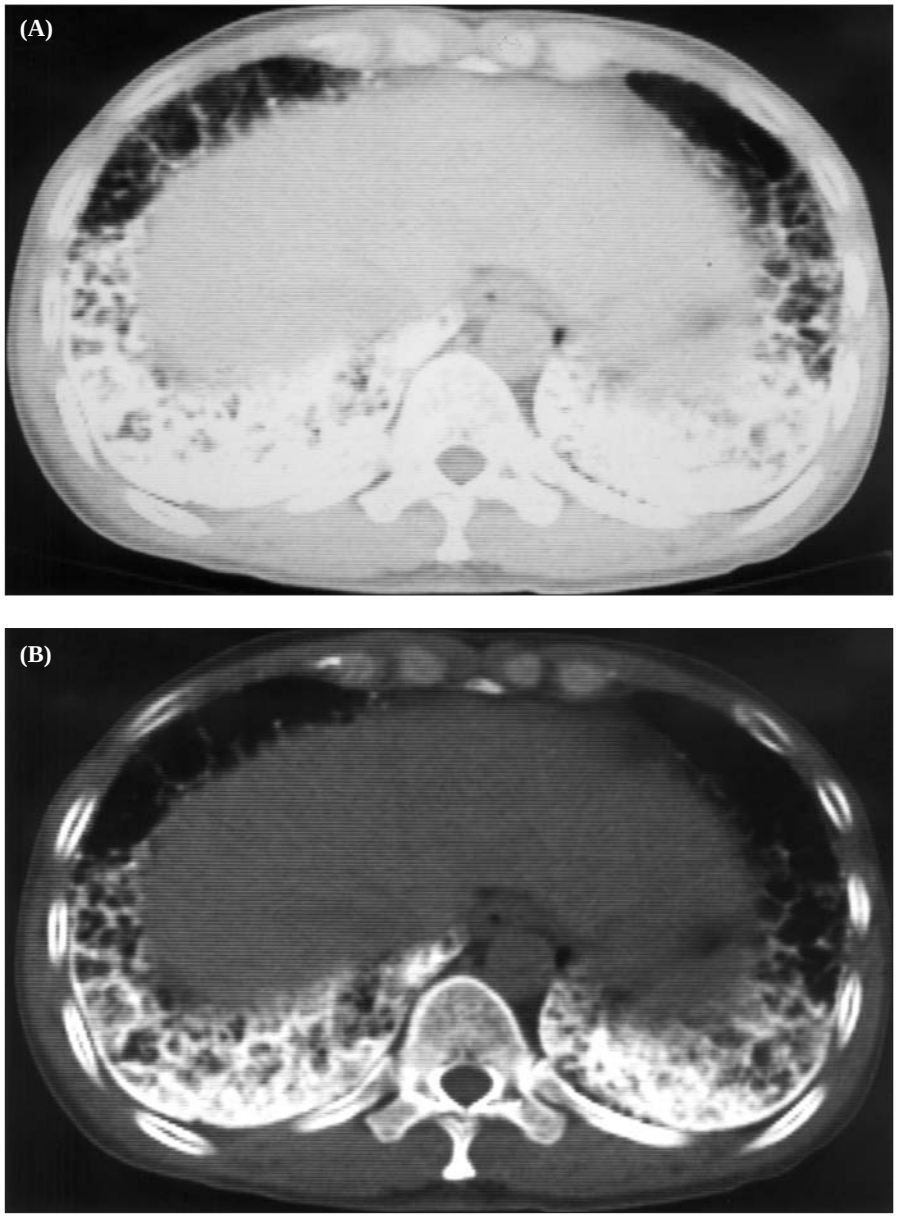

Fig. 4. - A 42-year-old man (slice thickness 10 mm).
(A) Window level –300, window width 1000. CT scan obtained at the level of the diaphragm demonstrates ground-glass opacities and consolidation.
(B) Window level 50, window width 1000. Calcification can be seen diffusely in the area of consolidation.

All patients had cysts, less than 10 mm in diameter, along the pleura and 1 cm to 8 cm diameter bullae in the apical regions. The subpleural cysts were shown to represent dilated alveolar ducts. Previous reports have shown that emphysematous bullae in apical areas may be associated with development of pneumothorax [5, 15, 16].

In the present study, calcified lines along the pleura were commonly seen on CT. *Sosman et al.* reported that the calcification is in the subpleural lung parenchyma rather than pleura [1], while *Winzelberg et al.* and *Chalmers et al.* described the presence of pleural calcification on CT [4, 5]. Autopsy specimens in two patients in the current study demonstrated small amounts of pleural calcification. They did demonstrate, however, numerous calcified nodules in the subpleural lung parenchyma. The autopsy findings in our two patients showed that the apparent pleural calcification seen on CT is due predominately to intraparenchymal subpleural calcospherites rather than pleural calcification.

Our study has several limitations. Firstly, the study was retrospective and included small number of patients. Secondly, evaluated CT scans were obtained at different institutions using different protocols. Thirdly, in this study the images with 10 mm collimation were mainly used. A 10 mm collimation is too thick to discuss the CT description of a diffuse lung disease. Finally, although it included a greater number of patients than in previous studies, all patients were more than 40 years old and had long-standing disease.

In conclusion, pulmonary alveolar microlithiasis is characterised by the presence of a myriad of fine calcified nodules and parenchymal calcifications along interlobular septa, broncho-vascular bundles and pleura on CT. Ground-glass attenuation, air-space consolidation, thickening of interlobular septa and bronchovascular bundles, and subpleural cysts are also common.

Reference

1. Sosman Mc, Dodd GD, Hones WD, U.Pillmore G. The familial occurrence of pulmonary alveolar microlithiasis. *Am J Roentgenol* 1957; 77: 947-1012.
2. Fraser RG, Pare JAP, Pare PD, Fraser RS, Genereux GP. Diagnosis of disease of the chest. Third ed. Philadelphia: WB Saundres; 1991.
3. Helbich TH, Wojnarovsky C, Wunderbaldinger P, Heinz-Peer G, Eichler I, Herold CJ. Pulmonary alveolar microlithiasis in children: radiographic and high-resolution CT findings. *Am J Roentgenol* 1997; 168: 63-5.
4. Cluzel P, Grenier P, Bernadac P, Laurent F, Picard JD. Pulmonary alveolar microlithiasis: CT findings. *J Comput Assist Tomogr* 1991; 15: 938-42.
5. Winzelberg GG, Boller M, Sachs M, Weinberg J. CT evaluation of pulmonary alveolar microlithiasis. *J Comput Assist Tomogr*1984; 8: 1029-31.
6. Chalmers AG, Wyatt J, Robinson PJ. Computed tomo-

graphic and pathological findings in pulmonary alveolar microlithiasis. *Br J Radiol* 1986; 59: 408-11.
7. Korn MA, Schurawitzki H, Klepetko W, Burghuber OC. Pulmonary alveolar microlithiasis: findings on high-resolution CT. *AJR Am J Roentgenol* 1992; 158: 981-2.
8. Schmidt H, Lorcher U, Kitz R, Zielen S, Ahrens P, Konig R. Pulmonary alveolar microlithiasis in children. *Pediatr Radiol* 1996; 26: 33-6.
9. Prakash UB, Barham SS, Rosenow EC, 3rd, Brown ML, Payne WS. Pulmonary alveolar microlithiasis. A review including ultrastructural and pulmonary function studies. *Mayo Clin Proc* 1983; 58: 290-300.
10. Cale WF, Petsonk EL, Boyd CB. Transbronchial biopsy of pulmonary alveolar microlithiasis. *Arch Intern Med* 1983; 143: 358-9.
11. Palombini BC, da Silva Porto N, Wallau CU, Camargo JJ. Bronchopulmonary lavage in alveolar microlithiasis. *Chest* 1981; 80: 242-3.
12. Balikian JP, Fuleihan FJ, Nucho CN. Pulmonary alveolar microlithiasis. Report of five cases with special reference to roentgen manifestations. *Am J Roentgenol Radium Ther Nucl Med* 1968; 103: 509-18.
13. Miro JM, Moreno A, Coca A, Segura F, Soriano E. Pulmonary alveolar microlithiasis with an unusual radiological pattern. *Br J Dis Chest* 1982; 76: 91-6.
14. Melamed JW, Sostman HD, Ravin CE. Interstitial thickening in pulmonary alveolar microlithiasis: an underappreciated finding. *J Thorac Imaging* 1994; 9: 126-8.
15. Shishido S, Toritani T, Nakano H, Tokushima T. [A case of alveolar microlithiasis which developed spontaneous pneumothorax due to progression of emphysematous bullae during 34 years after established diagnosis]. *Nihon Kyobu Shikkan Gakkai Zasshi* 1993; 31: 881-5.
16. Waters MH. Microlithiasis Alveolaris Pulmonum. *Tubercle* 1960; 41: 276-280.